

Learning Chebyshev Basis in Graph Convolutional Networks for Skeleton-based Action Recognition

Hichem Sahbi
CNRS Sorbonne University

◆

Abstract

Spectral graph convolutional networks (GCNs) are particular deep models which aim at extending neural networks to arbitrary irregular domains. The principle of these networks consists in projecting graph signals using the eigen-decomposition of their Laplacians, then achieving filtering in the spectral domain prior to back-project the resulting filtered signals onto the input graph domain. However, the success of these operations is highly dependent on the relevance of the used Laplacians which are mostly handcrafted and this makes GCNs clearly sub-optimal.

In this paper, we introduce a novel spectral GCN that learns not only the usual convolutional parameters but also the Laplacian operators. The latter are designed "end-to-end" as a part of a recursive Chebyshev decomposition with the particularity of conveying both the differential and the non-differential properties of the learned representations – with increasing order and discrimination power – without overparametrizing the trained GCNs. Extensive experiments, conducted on the challenging task of skeleton-based action recognition, show the generalization ability and the outperformance of our proposed Laplacian design w.r.t. different baselines (built upon handcrafted and other learned Laplacians) as well as the related work.

1 INTRODUCTION

Deep learning is currently witnessing a major interest in computer vision and different related fields [3], [6], [10], [20], [77]–[79], [144], [150]. Its principle consists in training multi-layered neural networks by designing suitable architectures and optimizing their parameters [92]. In particular, convolutional networks are well studied and aim at extracting features that gradually capture *low-to-high* semantics of visual patterns. Early convolutional networks were dedicated to regular (grid-like) data such as images where convolutions are achieved by shifting equivariant filters and measuring their responses across different image locations. However, data sitting on top of irregular domains (such as skeletons in action recognition) require extending convolutional networks to graph data [94]–[97]; while shifting convolutional filters across regular grids is a straightforward and a well-defined operation, its extension to irregular domains (namely graphs with heterogeneous topological properties) is known to be generally *ill-posed*.

Motivated by the success of deep learning in computer vision and machine learning, graph convolutional networks (GCNs) are currently emerging for different use-cases and applications [98]. The common ground of these networks consists in aggregating node representations prior to apply convolutional filters on the resulting node aggregates [98], [103], [112]–[114], [116] (see also [34], [40], [48], [132], [138]). Two categories of GCNs are known in the literature: the first one, dubbed as spatial [30], [99]–[103], achieves convolution by *locally* averaging representations through nodes and their neighbors before applying convolutions using inner products. The second category, known as spectral [25], [28], [56], [94], [95], [97], [105]–[107], [109], proceeds differently by first mapping filter and input graph signals using the eigen-decomposition of their Laplacians, then achieving filtering in the resulting spectral domain prior to

back-project the filtered signal onto the graph domain [110], [111]. While spectral GCNs make convolutions well-defined compared to spatial GCNs, their downside resides in the non-localized aspect of the learned filters and also in the high complexity of Laplacian eigen-decomposition.

Other spectral GCNs, known as Chebyshev networks [95], consider instead localized convolutional filters using a recursive polynomial decomposition. The success of these particular networks relies on the relevance of the used Laplacian operators which are usually handcrafted or built upon the inherent properties of the targeted applications (e.g., node-to-node relationships in 3D skeletons). However, handcrafted Laplacians are not able to capture all the relationships between nodes as their setting is agnostic to the targeted tasks. For instance, when considering skeleton-based action recognition, pre-existing node-to-node relationships capture the intrinsic anthropometric aspects of individuals which are necessary for their identification, while other relationships, yet to infer, about their dynamics are necessary in order to recognize their actions (See Fig. 3). Put differently, depending on the task at hand, connectivity in Laplacian operators should be appropriately learned by including not only the available (intrinsic) node-node connections in graphs but also their inferred (extrinsic) relationships.

Current state-of-the art has shifted towards the learning of connectivity in graph signal processing [117], [119]–[123], [125], [126], [128], [130] and more recently in GCNs [46], [69], [131]. The principle of these methods consists in learning graph connectivity by including explicitly the properties of the underlying Laplacians during optimization [127]. Our proposed method in this paper is different at least in two aspects; on the one hand, none of this related work considers Laplacian learning as a part of Chebyshev basis design. On the other hand, existing methods consider multiple independent matrix operators that capture the actual topology of the input graphs and increase the discrimination power of the learned GCN representations, but this comes at the expense of overparametrized networks and the risk of overfitting. In contrast, our Chebyshev basis design increases the discrimination power of the representations (that capture different hops in graphs) without overparametrizing the trained networks as the learned Laplacian parameters are shared through all the Chebyshev polynomials. Besides, making the Chebyshev basis¹ orthogonal allows to control the actual number of training parameters and further enhances the generalization power of our GCNs as corroborated later in experiments.

In this paper, we introduce a novel framework that learns Laplacians as a part of GCN and Chebyshev basis design. This basis is expressed using an efficient recursive form evaluated on a single shared Laplacian operator which conveys both the differential and non-differential properties of the learned graph representations. This Chebyshev basis also captures the statistical properties of the learned representations, with increasing order and discrimination power, without increasing the actual number of training parameters in the resulting GCNs. Different settings are considered in our design including symmetry and orthogonality that further constrain the learned Laplacians and enhance the generalization capacity of our GCNs. Experiments, conducted on the challenging task of skeleton-based action and hand-gesture recognition show the high accuracy and the outperformance of our method w.r.t. different baselines as well as the related work.

2 RELATED WORK

In this section, we discuss the related work both from the methodological and the application point-of-view. This includes graph and Laplacian inference as well as skeleton-based action recognition.

Graph and Laplacian inference. Laplacian inference (or equivalently graph design) is generally ill-posed, NP-hard [1], [2], [4] and most of the existing approaches rely on constraints (similarity, smoothness, sparsity, band-limitedness, etc. [117], [119]–[123], [125]–[128], [130]) for its conditioning [5], [7]. Particularly in GCNs, early methods [97], [100] rely on handcrafted or predetermined node-to-node relationships using similarities or the inherent properties of the targeted applications in order to define Laplacian operators [8],

1. The generative aspect of our basis makes it possible to capture different hops of neighbors without increasing the actual number of training parameters and this enhances the discrimination power of the learned representation as shown through this paper.

[97]. However, in spite of being relatively effective, the potential of these operators is not fully explored as their design is either agnostic to the tasks at hand or achieved using the tedious cross validation. More recent advances aim at defining graph topology that best fits a given task [9], [11], [12], [14], [15], [17], [28], [107]. For instance, the work in [15] proposes a graph network for semi-supervised classification that learns graph topology with sparse structure given a cloud of points; node-to-node connections are modeled with a joint probability distribution on Bernoulli random variables whose parameters are found using bi-level optimization. A computationally more efficient variant is introduced in [17] using a weighted cosine similarity and edge thresholding. Other solutions make improvement w.r.t. the original GCNs [97] by exploiting symmetric matrices [28] and discovering hidden structural relations (unspecified in the original graphs), using a so-called residual graph adjacency matrix and by learning a distance function over nodes. The work in [107] introduces a dual architecture with two parallel graph convolutional layers sharing the same parameters. This method considers a normalized adjacency matrix and a positive pointwise mutual information matrix to capture node co-occurrences through random walks sampled from graphs.

Skeleton-based action modeling. Action recognition is one of the main challenging tasks in computer vision [52], [58], [124] which has been tackled using RGB-based [51], depth-based [49] and skeleton-based techniques [50]. In particular, with the emergence of sensors (including Intel RealSense [43] and Microsoft Kinect [45]), interest in pose estimation and skeleton-based action recognition is increasingly growing [53]. Early skeleton-based methods are based on modeling human motions using handcrafted features [39], [41], time series and dynamic time warping [38] as well as Fourier temporal pyramids [68]. However, most of these techniques are oblivious to the interactions that may exist between the most relevant body parts, i.e., those which are actually involved in human actions. Other solutions model these interactions [71]–[73] using skeletal quad [75], Lie group [38] and temporal relationships [76]. With the resurgence of deep learning [77]–[79], all these methods have been quickly overtaken by convolutional and recurrent neural networks [29], [42], [51], [80], [82], [83], [86] as well as their LSTM variants [32], [33], [35], [37], [84], [86], [87], and some of them rely on attention mechanisms that focus on the most relevant joints in skeletons [31], [88]. With the recent emergence of GCNs [55]–[57] particularly in skeleton-based action recognition [19], [26], [47], [54], [66], [67], [90], [91], these models have been increasingly used for this task as they explicitly model, with a better interpretability, the spatial and temporal interaction among joints either separately [47] or jointly [46]. However, while all joints contribute in motion, only a few of them are actually relevant to recognize the targeted action categories; hence, other work focuses on learning more complete spatial and temporal co-occurrences for skeleton data [28], [59], [65], [69].

In all the aforementioned work, none of the existing methods considers the issue of learning connectivity in graphs and Laplacians as a part of Chebyshev GCN design and this constitutes the main contribution of the following sections.

3 CHEBYSHEV CONVOLUTIONAL NETWORKS

Let $\mathcal{S} = \{\mathcal{G}_i = (\mathcal{V}_i, \mathcal{E}_i)\}_i$ denote a collection of graphs with $\mathcal{V}_i, \mathcal{E}_i$ being respectively the nodes and the edges of \mathcal{G}_i . Each graph \mathcal{G}_i (denoted for short as $\mathcal{G} = (\mathcal{V}, \mathcal{E})$) is endowed with a graph signal $\{\psi(u) \in \mathbb{R}^s : u \in \mathcal{V}\}$ and associated with an adjacency matrix \mathbf{A} with each entry $\mathbf{A}_{uu'} > 0$ iff $(u, u') \in \mathcal{E}$ and 0 otherwise; as shown later in Section 5.1, $\psi(v)$ corresponds to the motion feature of skeletons. Our goal is to design a GCN that returns the representation and the classification of a given graph using a novel design of Laplacian convolution on graphs as shown subsequently.

Given a graph $\mathcal{G} = (\mathcal{V}, \mathcal{E})$ with $|\mathcal{V}| = n, |\mathcal{E}|$ being respectively the number of its vertices and edges and \mathbf{L} the Laplacian of \mathcal{G} ; for instance, \mathbf{L} could be the random walk defined as $\mathbf{L} = \mathbf{I}_n - \mathbf{A}[\mathbf{D}^{-1}(\mathbf{A})]$ where \mathbf{I}_n is an $n \times n$ identity matrix and $\mathbf{D}(\mathbf{A})$ a diagonal degree matrix with each diagonal entry $[\mathbf{D}(\mathbf{A})]_{uu} = \sum_v \mathbf{A}_{vu}$. Let $\mathbf{U}\mathbf{A}\mathbf{U}^\top$ be the eigen-decomposition of \mathbf{L} , with $\mathbf{U}, \mathbf{\Lambda}$ being respectively the matrix of eigenvectors

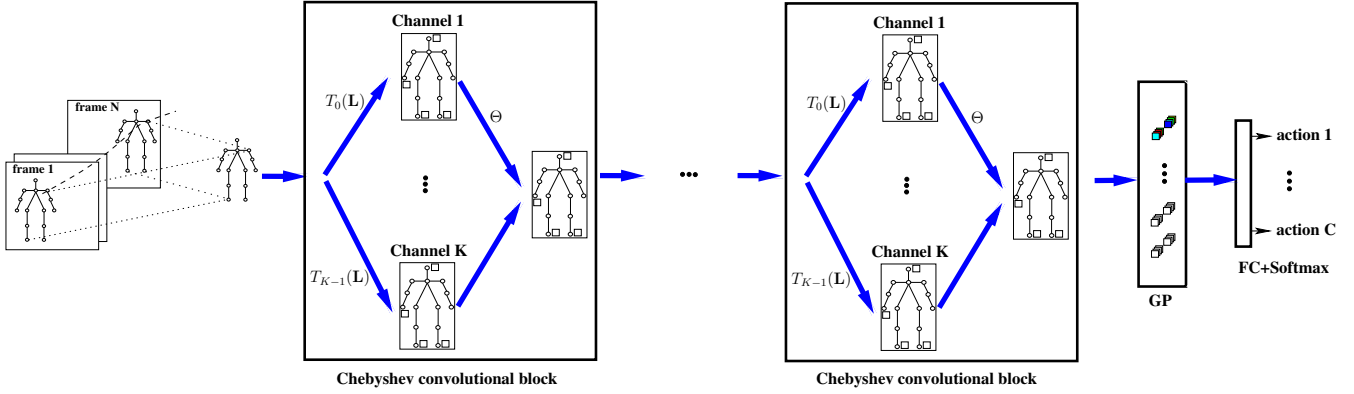


Fig. 1. This figure shows the architecture of our Chebyshev Convolutional Network. In each convolutional block, the Chebyshev basis $\{T_k(\cdot)\}_k$ is first evaluated on the Laplacian \mathbf{L} , then multiplied by the input graph signal $\psi(\mathcal{V})$, and finally aggregated using the parameters in Θ . These Chebyshev convolutional blocks are followed by global average pooling prior to softmax classification. Note that the Laplacian \mathbf{L} is shared across the basis $\{T_k(\cdot)\}_k$ and through the Chebyshev convolutional blocks. (Better to zoom the pdf).

(graph Fourier basis) and the diagonal matrix of its eigenvalues; spectral graph convolution is a well defined operator (see for instance [98]) which is achieved by first projecting a given graph signal $\psi(\cdot)$ using the eigen-decomposition of \mathbf{L} , and then multiplying the resulting projection by a convolutional filter prior to back-project the result in the original signal space.

Formally, the convolutional operator $\star_{\mathcal{G}}$ (rewritten for short as \star) on a given graph signal $\psi(\mathcal{V}) \in \mathbb{R}^{s \times n}$ is $(\psi \star g_{\theta})_{\mathcal{V}} = \mathbf{U} g_{\theta}(\Lambda) \mathbf{U}^{\top} \psi(\mathcal{V})^{\top}$; here \top is the matrix transpose operator and g_{θ} denotes a non-parametric convolutional filter defined as $g_{\theta}(\Lambda) = \text{diag}(\theta)$ with $\theta \in \mathbb{R}^n$. As this filter is non-localized, we consider instead [95]

$$(\psi \star g_{\theta})_{\mathcal{V}} = \sum_{k=0}^{K-1} T_k(\mathbf{L}) \psi(\mathcal{V})^{\top} \theta_k, \quad (1)$$

with $\theta = (\theta_0 \dots \theta_{K-1})^{\top} \in \mathbb{R}^K$ being the learned convolutional filter parameters and T_k the k -th order Chebyshev polynomial recursively defined as $T_k(\mathbf{L}) = 2\mathbf{L} \circ T_{k-1}(\mathbf{L}) - T_{k-2}(\mathbf{L})$, with $T_k(\mathbf{L}) \in \mathbb{R}^{n \times n}$, $T_0(\mathbf{L}) = \mathbf{I}_n$, $T_1(\mathbf{L}) = \mathbf{L}$ and \circ the hadamard (element-wise) matrix product. When \mathbf{L} is the combinatorial Laplacian, we consider in practice a rectified version as $2\mathbf{L}/\lambda_{\max} - \mathbf{I}_n$ (instead of \mathbf{L} with λ_{\max} being the largest eigenvalue of \mathbf{L}) in order to guarantee the orthogonality of the basis $\{T_k(\mathbf{L})\}_k$; see again [95] and later (in section 4.2) the general rectification of any Laplacian that guarantees orthogonality of the Chebyshev basis.

Using Eq. 1, the extension of convolution to multiple filters $\mathcal{F} = \{g_{\theta}\}_{\theta}$ and $|\mathcal{V}|$ nodes can be written as

$$(\psi \star \mathcal{F})_{\mathcal{V}} = \sum_{k=0}^{K-1} T_k(\mathbf{L}) \psi(\mathcal{V})^{\top} \Theta_k, \quad (2)$$

here $\Theta = (\Theta_k)_{k=0}^{K-1}$ is the matrix of convolutional parameters associated to multiple channels (filters). In Eq. 2, the input signal $\psi(\mathcal{V})$ is projected using the Chebyshev polynomials $\{T_k(\mathbf{L})\}_k$; in particular, when $k = 1$, $T_k(\mathbf{L}) = \mathbf{L}$ and this provides for each node u , the aggregate set of its neighbors. Taking high order polynomials capture the k hop neighbor aggregates in \mathcal{V} and makes it possible to model larger extents and more influencing contexts. When the Laplacian \mathbf{L} is common to all the graphs and also shared between $\{T_k(\cdot)\}_k$, entries of \mathbf{L} could be handcrafted or learned, so Eq. 2 implements a Chebyshev convolutional block with two layers; the first one aggregates signals in $\mathcal{N}_k(\mathcal{V})$ by multiplying $\psi(\mathcal{V})$ by $\{T_k(\mathbf{L})\}_k$ while the second layer achieves convolution by multiplying the resulting aggregate signals by the filter parameters in Θ . The whole architecture of this convolution is described in Fig. 1.

Constraints	Parametrization	Jacobian
COMB	$\mathbf{D}(\mathbf{A}^\top) - \mathbf{A}$	$[\mathbf{J}_c]_{ij,pq} = 1_{\{i=j,p \neq q\}} - 1_{\{i \neq j\}}$
NDRW	$\mathbf{A} \cdot [\mathbf{D}(\mathbf{A})]^{-1}$	$[\mathbf{J}_{ndrw}]_{ij,pq} = 1_{\{j=q\}} \cdot (\delta_{ip} - \mathbf{L}_{ij}) \cdot [\mathbf{1}_n \cdot \mathbf{D}(\mathbf{A})^{-1}]_{pq}$
DRW	$\mathbf{I}_n - \mathbf{A} \cdot [\mathbf{D}(\mathbf{A})]^{-1}$	$[\mathbf{J}_{drw}]_{ij,pq} = 1_{\{j=q\}} \cdot (\mathbf{L}_{ij} - \delta_{ip}) \cdot [\mathbf{1}_n \cdot \mathbf{D}(\mathbf{A})^{-1}]_{pq}$
NDN	$[\mathbf{D}(\mathbf{A}^\top)]^{-\frac{1}{2}} \mathbf{A} \cdot [\mathbf{D}(\mathbf{A})]^{-\frac{1}{2}}$	$[\mathbf{J}_{ndn}]_{ij,pq} = 1_{\{i=p \vee j=q\}} \cdot \frac{\mathbf{L}_{ij}}{2\mathbf{A}_{pq}} \cdot (2\delta_{ip}\delta_{jq} - [\mathbf{D}(\mathbf{A}^\top)]^{-1} \mathbf{A} + \mathbf{A} \mathbf{D}(\mathbf{A})^{-1})_{pq}$
DN	$\mathbf{I}_n - [\mathbf{D}(\mathbf{A}^\top)]^{-\frac{1}{2}} \mathbf{A} \cdot [\mathbf{D}(\mathbf{A})]^{-\frac{1}{2}}$	$[\mathbf{J}_{dn}]_{ij,pq} = 1_{\{i=p \vee j=q\}} \cdot \frac{\mathbf{L}_{ij}}{2\mathbf{A}_{pq}} \cdot ([\mathbf{D}(\mathbf{A}^\top)]^{-1} \mathbf{A} + \mathbf{A} \mathbf{D}(\mathbf{A})^{-1})_{pq} - 2\delta_{ip}\delta_{jq}$
Symmetry	$\mathbf{A} + \mathbf{A}^\top$	$[\mathbf{J}_s]_{ij,pq} = 1_{\{(i=p,j=q) \vee (i=q,j=p)\}}$
S-COMB	$\mathbf{D}(\mathbf{A} + \mathbf{A}^\top) - (\mathbf{A} + \mathbf{A}^\top)$	$\mathbf{J}_{sc} = \mathbf{J}_c \cdot \mathbf{J}_s$
S-NDRW	$(\mathbf{A} + \mathbf{A}^\top) \cdot [\mathbf{D}(\mathbf{A} + \mathbf{A}^\top)]^{-1}$	$\mathbf{J}_{sdrw} = \mathbf{J}_{ndrw} \cdot \mathbf{J}_s$
S-DRW	$\mathbf{I}_n - (\mathbf{A} + \mathbf{A}^\top) \cdot [\mathbf{D}(\mathbf{A} + \mathbf{A}^\top)]^{-1}$	$\mathbf{J}_{sdrw} = \mathbf{J}_{drw} \cdot \mathbf{J}_s$
S-NDN	$[\mathbf{D}(\mathbf{A} + \mathbf{A}^\top)]^{-\frac{1}{2}} (\mathbf{A} + \mathbf{A}^\top) \cdot [\mathbf{D}(\mathbf{A} + \mathbf{A}^\top)]^{-\frac{1}{2}}$	$\mathbf{J}_{sndn} = \mathbf{J}_{ndn} \cdot \mathbf{J}_s$
S-DN	$\mathbf{I}_n - [\mathbf{D}(\mathbf{A} + \mathbf{A}^\top)]^{-\frac{1}{2}} (\mathbf{A} + \mathbf{A}^\top) \cdot [\mathbf{D}(\mathbf{A} + \mathbf{A}^\top)]^{-\frac{1}{2}}$	$\mathbf{J}_{sdn} = \mathbf{J}_{dn} \cdot \mathbf{J}_s$

TABLE 1

Different parametrizations and the underlying Jacobians. In this table, COMB stands for ‘‘Combinatorial’’ Laplacian, NDRW for ‘‘Non Differential Random Walk’’, DRW for ‘‘Differential Random Walk’’, NDN for ‘‘Non Differential Normalized’’ Laplacian, and DN for ‘‘Differential Normalized’’ one. The symmetric variants of these Laplacians are prefixed by ‘‘S’’.

4 OUR CHEBYSHEV BASIS DESIGN

The success of the aforementioned convolutional process is highly dependent on the relevance of the Laplacian \mathbf{L} and knowing a priori which Laplacian (and its hyper-parameters) to choose could be challenging and usually relies on the tedious cross-validation. One may consider a solution that learns convex combinations of individual Laplacians, each one dedicated to a particular topology of input graph data. However (and as also supported later by experiments), this solution is limited by the modeling capacity of individual Laplacians; in other words, *if none of the individual Laplacians capture the actual topology of the input graphs, then their combinations may also be limited to fully capture this topology*. Our contribution in this paper aims, rather, at designing convolutional Laplacian operators (‘‘from scratch’’) by learning the topological structure of the input graphs.

Considering the tensor of the Chebyshev polynomials $\{T_k(\mathbf{L})\}_k$ and following Eq 2, the operations in $\{T_k(\mathbf{L})\psi(\mathcal{V})^\top\}_k$ act as feature extractors that collect different order statistics (including means and variances) of nodes and their neighbors. For instance, when $\mathbf{L} = \mathbf{A}[\mathbf{D}(\mathbf{A})]^{-1}$ then $T_1(\mathbf{L})\psi(\mathcal{V})^\top$ models expectations $\{\mathbb{E}(\psi(\mathcal{N}_k(u)))\}_u$ and if one considers instead $\mathbf{L} = \mathbf{I}_n - \mathbf{A}[\mathbf{D}(\mathbf{A})]^{-1}$ then $T_1(\mathbf{L})\psi(\mathcal{V})^\top$ captures, up to a square power, the statistical variance $\{\psi(u) - \mathbb{E}(\psi(\mathcal{N}_k(u)))\}_u$. Hence, $\{T_k(\mathbf{L})\}_k$ corresponds to a basis that extracts different order statistics of graph signals before convolution.

Let \mathcal{L} denote the cross entropy loss associated to a given classification task. We turn the design of the Laplacian operator \mathbf{L} (thereby $\{T_k(\mathbf{L})\}_k$) as a part of GCN training; considering the gradient of \mathcal{L} w.r.t. the Chebyshev terms, denoted as $\nabla_k \mathcal{L} = \frac{\partial \mathcal{L}}{\partial T_k(\mathbf{L})}$, and since \mathbf{L} is shared across $\{T_k(\mathbf{L})\}_k$, one may obtain

$$\frac{\partial \mathcal{L}}{\partial \mathbf{L}} = \mathbf{vec}^{-1} \left(\sum_{k=0}^{K-1} \mathbf{J}_k \cdot \mathbf{vec}(\nabla_k \mathcal{L}) \right), \quad (3)$$

being $\mathbf{J}_k \in \mathbb{R}^{n^2 \times n^2}$ the diagonal Jacobian matrix whose entry $[\mathbf{J}_k]_{ij,ij} = \frac{\partial [T_k(\mathbf{L})]_{ij}}{\partial \mathbf{L}_{ij}}$ and $\mathbf{vec}(\cdot)$ a vectorization that appends the entries of a given matrix using the x-y order in \mathbf{J}_k , and \mathbf{vec}^{-1} its inverse. In the above equation, one may show that $\frac{\partial [T_k(\mathbf{L})]_{ij}}{\partial \mathbf{L}_{ij}}$ can be recursively obtained as

$$\begin{cases} 0 & k = 0 \\ 1 & k = 1 \\ 2 \left[[T_{k-1}(\mathbf{L})]_{ij} + \mathbf{L}_{ij} \frac{\partial [T_{k-1}(\mathbf{L})]_{ij}}{\partial \mathbf{L}_{ij}} \right] - \frac{\partial [T_{k-2}(\mathbf{L})]_{ij}}{\partial \mathbf{L}_{ij}} & k \geq 2, \end{cases} \quad (4)$$

so \mathbf{L} can be updated using Eqs (3), (4) and stochastic gradient descent (SGD).

4.1 Constraining the Laplacian

As described above, the learned matrix \mathbf{L} is not guaranteed to be a valid Laplacian². In order to further constrain \mathbf{L} to be a valid Laplacian, \mathbf{L} is reparametrized as $\mathbf{L} = \mathbf{D}(\mathbf{A}) - \mathbf{A}$ which corresponds to the combinatorial form of the Laplacian. If one further constrains \mathbf{A} to be column-stochastic, then \mathbf{L} corresponds to the random walk graph Laplacian which captures the differential properties of graphs; a variant of this operator, dubbed as normalized, is defined as $\mathbf{L} = \mathbf{I}_n - [\mathbf{D}(\mathbf{A}^\top)]^{-\frac{1}{2}} \mathbf{A} [\mathbf{D}(\mathbf{A})]^{-\frac{1}{2}}$. Note that omitting the left-hand side terms (in the aforementioned Laplacians) makes it possible to capture the non-differential properties in graphs.

With this parametrization of \mathbf{L} , one may turn the design of \mathbf{L} into the learning of \mathbf{A} while guaranteeing the resulting matrix \mathbf{L} to be a valid Laplacian. If one further constrains \mathbf{A} to be symmetric, then all the learned Laplacians will have real eigenvalues and some of them positive semi-definite [111]; these properties are important when handling undirected graphs and also in Laplacian regularization [148]. Considering these settings of \mathbf{L} , the chain rule leads to

$$\frac{\partial \mathcal{L}}{\partial \mathbf{A}} = \text{vec}^{-1} \left(\mathbf{J} \cdot \text{vec} \left(\frac{\partial \mathcal{L}}{\partial \mathbf{L}} \right) \right), \quad (5)$$

with $\frac{\partial \mathcal{L}}{\partial \mathbf{L}}$ obtained from Eq. 3 and \mathbf{J} being a sparse Jacobian matrix whose entry $[\mathbf{J}]_{ij,pq} = [\frac{\partial \mathbf{L}_{ij}}{\partial \mathbf{A}_{pq}}]_{ij,pq}$; this matrix is given in table 1 for different Laplacian settings including the combinatorial and random walk which capture the differential and non-differential properties of node features. We also consider the differential random walk – as a combination these two Laplacians – obtained by plugging the latter into the former. All these Laplacians are built upon either symmetric or non-symmetric matrices \mathbf{A} . Note that symmetry is obtained using weight sharing, i.e., by constraining the upper and the lower triangular parts of \mathbf{A} to share the same entries. This is guaranteed by considering a reparametrization as $\mathbf{A} + \mathbf{A}^\top$ (with \mathbf{A} being now a free matrix) and by tying pairwise symmetric entries of the gradient $\frac{\partial \mathcal{L}}{\partial \mathbf{A}}$; this is equivalently obtained by multiplying the original gradient $\frac{\partial \mathcal{L}}{\partial \mathbf{A}}$ by the Jacobian $[\mathbf{J}_s]_{ij,pq} = 1_{\{(i=p,j=q) \vee (i=q,j=p)\}}$ which is again extremely sparse and its evaluation is highly efficient.

4.2 Orthogonality

Learning multiple matrices $\{T_k(\mathbf{L})\}_{k=0}^{K-1}$ allow us to capture different graph topologies when achieving aggregation and convolution, and this enhances the discrimination power of the GCN representations without increasing the actual number of training parameters (as also shown later in experiments). However, if aggregation produces, for a given $u \in \mathcal{V}$, linearly dependent vectors $\mathcal{X}_u = \{\sum_{u'} [T_k(\mathbf{L})]_{uu'} \cdot \psi(u')\}_k$, then convolution will also generate linearly dependent representations with an overestimated number of training parameters in the null space of \mathcal{X}_u . Besides, matrices $\{T_1(\mathbf{L}), \dots, T_K(\mathbf{L})\}$ used for aggregation, may also correspond to overlapping and redundant neighborhoods.

Provided that $\{\psi(u')\}_{u' \in \mathcal{N}_r(u)}$ are linearly independent, and K upper-bounded by $\text{rank}(\{\psi(u')\}_{u' \in \mathcal{N}_r(u)}) \leq \min(|\mathcal{V}|, s)$, the condition that makes vectors in \mathcal{X}_u linearly independent reduces to orthogonality, i.e., $\langle T_k(\mathbf{L}), T_{k'}(\mathbf{L}) \rangle_F = 0, \forall k \neq k'$, with $\langle \cdot, \cdot \rangle_F$ being the Hilbert-Schmidt (or Frobenius) inner product defined as $\langle T_k(\mathbf{L}), T_{k'}(\mathbf{L}) \rangle_F = \text{tr}(T_k(\mathbf{L})^\top T_{k'}(\mathbf{L}))$ with $\text{tr}(\cdot)$ being the matrix trace operator. A sufficient condition that guarantees the orthogonality of the Chebyshev basis consists in taking the Laplacian $2(\mathbf{L} - \lambda_{\min} \mathbf{I}_n) / (\lambda_{\max} - \lambda_{\min}) - \mathbf{I}_n$ instead of \mathbf{L} with λ_{\min} (resp. λ_{\max}) being the smallest (resp. largest) eigenvalue of \mathbf{L} , and this guarantees that the eigenvalues of the resulting matrix to be in $[-1, +1]$ and hence the orthogonality (minimality) of $\{T_k(\mathbf{L})\}_k$ (see for instance [95]). It is easy to see that this normalization equates the rectified Laplacian shown in section 3 (i.e., on the combinatorial setting) as its smallest eigenvalue is zero.

2. See for instance [127] for a comprehensive review of the properties of valid Laplacian operators.

5 EXPERIMENTS

In this section, we evaluate the performance of our GCN network on the task of action recognition using two challenging skeleton datasets; SBU Interaction [134] and First-Person Hand Action (FPHA) [133]. The purpose is to show the relevance of our Laplacian design and its comparison against different handcrafted Laplacians and learned ones as well as more general related work in action recognition.

5.1 Datasets and implementation details

Dataset description. SBU is an interaction dataset acquired (under relatively well controlled conditions) using the Microsoft Kinect sensor; it includes in total 282 moving skeleton sequences (performed by two interacting individuals) belonging to 8 categories: “approaching”, “departing”, “pushing”, “kicking”, “punching”, “exchanging objects”, “hugging”, and “hand shaking”. Each pair of interacting individuals corresponds to two 15 joint skeletons and each joint is encoded with a sequence of its 3D coordinates across video frames. In this dataset, we consider the same evaluation protocol as the one suggested in the original dataset release [134] (i.e., train-test split).

The FPHA dataset includes 1175 skeletons belonging to 45 action categories which are performed by 6 different individuals in 3 scenarios. In contrast to SBU, action categories are highly variable with inter and intra subject variability including style, speed, scale and viewpoint. Each skeleton includes 21 hand joints and each joint is again encoded with a sequence of its 3D coordinates across video frames. We evaluate the performance of our method using the 1:1 setting proposed in [133] with 600 action sequences for training and 575 for testing. In all these experiments, we report the average accuracy over all the classes of actions.

Skeleton normalization. Let $S^t = \{p_1^t, \dots, p_n^t\}$ denote the 3D skeleton coordinates at frame t . Without a loss of generality, we consider a particular order so that p_1^t , p_2^t and p_3^t correspond to three reference joints (e.g., neck, left shoulder and right shoulder for SBU dataset); as shown in Fig. 3, this corresponds to joints 2, 4 and 7 for SBU and 1, 3 and 5 for FPHA. As the relative distance between these 3 joints is stable w.r.t. any motion, these 3 joints are used in order to estimate the rigid motion (similarity transformation) for skeleton normalization (see also [135]). Each graph sequence is processed in order to normalize its 3D coordinates using a similarity transformation; the translation parameters $\mathbf{t} = (t_x, t_y, t_z)$ of this transformation correspond to the shift that makes the reference point $(p_2^0 + p_3^0)/2$ coincide with the origin while the rotation parameters $(\theta_x, \theta_y, \theta_z)$ are chosen in order to make the plane formed by p_1^0 , p_2^0 and p_3^0 coplanar with the x-y plane and the vector $p_2^0 - p_3^0$ colinear with the x-axis. Finally, the scaling γ of this similarity is chosen to make the $\|p_2^0 - p_3^0\|_2$ constant through all the action instances. Hence, each normalized joint is transformed as $\hat{p}_i^t = \gamma(p_i^t - \mathbf{t})R_x(\theta_x)R_y(\theta_y)R_z(\theta_z)$ with R_x , R_y , R_z being rotation matrices along x , y and z axis respectively.

Input graphs. Considering a sequence of normalized skeletons $\{S^t\}_t$, each joint sequence $\{\hat{p}_j^t\}_t$ in these skeletons defines a labeled trajectory through successive frames (see Fig. 2). Given a finite collection of trajectories, we consider the input graph $\mathcal{G} = (\mathcal{V}, \mathcal{E})$ where each node $v_j \in \mathcal{V}$ corresponds to the labeled trajectory $\{\hat{p}_j^t\}_t$ and an edge $(v_j, v_i) \in \mathcal{E}$ exists between two nodes iff the underlying trajectories are spatially neighbors. Each trajectory (i.e., node in \mathcal{G}) is processed using *temporal chunking*: first, the total duration of a sequence (video) is split into M equally-sized temporal chunks ($M = 4$ in practice), then the normalized joint coordinates $\{\hat{p}_j^t\}_t$ of the trajectory v_j are assigned to the M chunks (depending on their time stamps) prior to concatenate the averages of these chunks; this produces the description of v_j (again denoted as $\psi(v_j) \in \mathbb{R}^s$ with $s = 3 \times M$) and $\{\psi(v_j)\}_j$ constitutes the raw description of nodes in a given sequence. Note that two trajectories v_j and v_i , with similar joint coordinates but arranged differently in time, will be considered as very different when using temporal chunking. Note also that beside being compact and discriminant, this temporal chunking gathers advantages – while discarding drawbacks – of two widely used families of techniques mainly *global averaging techniques* (invariant but less discriminant) and

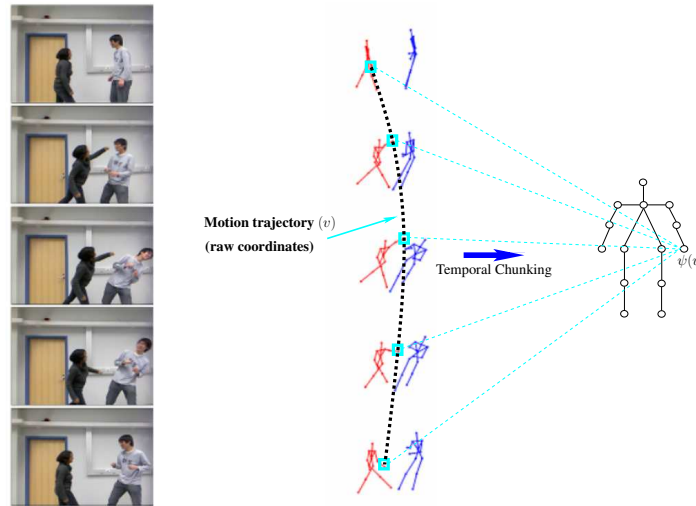


Fig. 2. This figure shows the whole keypoint tracking and description process.

frame resampling techniques (discriminant but less invariant). Put differently, temporal chunking produces discriminant raw descriptions that preserve the temporal structure of trajectories while being *frame-rate* and *duration* agnostic.

Implementation settings. We trained the GCN networks end-to-end using the Adam optimizer [147] for 1,800 epochs with a batch size equal to 200 for SBU and 600 for FPFA, a momentum of 0.9 and a global learning rate (denoted as $\nu(t)$) inversely proportional to the speed of change of the cross entropy loss used to train our networks; when this speed increases (resp. decreases), $\nu(t)$ decreases as $\nu(t) \leftarrow \nu(t-1) \times 0.99$ (resp. increases as $\nu(t) \leftarrow \nu(t-1)/0.99$). All these experiments are run on a GeForce GTX 1070 GPU device (with 8 GB memory) and neither dropout nor data augmentation are used.

5.2 Baselines

We compare the performances of our GCN w.r.t. different Chebyshev basis settings which are defined upon handcrafted and learned Laplacians, as well as against totally learned Laplacian basis. Note that all these Laplacians are combined with symmetry and orthogonality constraints as described earlier.

Handcrafted Laplacians (HL). All the Chebyshev terms $\{T_k(\cdot)\}_k$ are evaluated upon a *handcrafted* Laplacian \mathbf{L} which in turns depends on a fixed adjacency matrix \mathbf{A} (set using the original input graph).

Multi-Laplacians (ML). In this configuration, the Laplacian used in the Chebyshev terms is trained as a weighted *combination* of the handcrafted variants of the Laplacians in table 1 (built upon the fixed matrix \mathbf{A}). Note that orthogonality is obtained by normalizing the final learned Laplacian operator while symmetry is enforced in the handcrafted adjacency matrix \mathbf{A} .

Totally Learned Laplacians (TLL). In this variant, K independent Laplacians $\{\mathbf{L}_k\}_k$ (and hence the underlying adjacency matrices) are learned. In contrast to the handcrafted setting, orthogonality and symmetry as obtained as a part of the optimization process (as already discussed in sections 4.1 and 4.2).

5.3 Ablation study and comparison

Tables 2, 3 show a comparison of our GCN-based action recognition against the aforementioned GCN baselines, i.e. based on Handcrafted Laplacians and Totally Learned ones (performances with Multi-Laplacians are rather shown in Table 5); these comparisons are shown for different $K \in \{2, 4, 8\}$. From all these results, we observe a clear gain of our Chebyshev-based Laplacian design w.r.t. these baselines; at least one of the setting (namely $K = 4$) provides a significant gain. Table 4 shows an ablation study, where the impact of each component of our GCN (Laplacians, symmetry and orthogonality) is observed separately and jointly. From these results, we observe a positive impact when constraining the learned matrices to be symmetric and orthogonal; this gain is noticeable with non-differential Laplacians on SBU and with combined (differential/non-differential) ones on FPFA and this clearly shows the complementary aspect of these two Laplacian settings mainly on challenging datasets (i.e., FPFA). Again, this gain reaches the highest values when K is sufficiently (not very) large and this follows the small size of the original skeletons (diameter and dimensionality of the graphs and the signal) used for action recognition which constrains the required number of Laplacian terms in the Chebyshev decomposition. Hence, with few Chebyshev terms, our method is able to learn relevant Laplacians and representations for action recognition.

Our proposed Laplacian design avoids the strong bias about the handcrafted adjacency matrices which are rather suitable to capture the anthropometric characteristics of skeletons and less optimal for action recognition. On another hand, Tables. 2, 3 and 4 show that our Laplacian design makes it possible to capture better the topology of the graph data (i.e., the neighborhood system defined by the learned Laplacian and its underlying adjacency matrix \mathbf{A}). In contrast, the baselines are limited when connectivity is handcrafted and also when learned using totally trained Laplacians, as this results either into a biased Laplacian or into a larger number of training parameters, while Chebyshev provides a compromise between these two extreme cases. Indeed, it enhances the discrimination power of the representation without increasing the actual number of training parameters. In sum, the gain of our GCN results from (i) the relative flexibility of the proposed design which allows learning complementary aspects of graph topology (through the Chebyshev basis), and also (ii) the regularization effect of our constraints (Laplacian weight sharing in Chebyshev, Laplacian parametrization, orthogonality and symmetry) which mitigate overfitting.

Finally, we compare the classification performances of our GCN against other related methods in action recognition ranging from sequence based such as LSTM and GRU [32], [136], [151] to deep graph (non-vectorial) methods [46], etc. (see tables 5 and 6 and references within). From the results in these tables, our GCN brings a noticeable gain w.r.t. related state of the art methods.

Laplacians Settings		Differential COMB	Non-Differential NDRW NDN		Combined DRW DN	
$K = 2$	HL	96.9231	96.9231	96.9230	93.8462	96.9230
	TLL	96.9231	95.3846	98.4615	96.9231	98.4615
	Our	98.4615	98.4615	96.9230	96.9231	98.4615
$K = 4$	HL	95.3846	93.8462	96.9231	96.9230	96.9230
	TLL	96.9231	95.3846	98.4615	98.4615	96.9230
	Our	98.4615	100.000	98.4615	98.4615	98.4615
$K = 8$	HL	96.9231	98.4615	96.9231	96.9230	96.9230
	TLL	96.9231	98.4615	98.4615	93.8462	96.9230
	Our	96.9231	98.4615	98.4615	98.4615	98.4615

TABLE 2

Detailed performances on SBU using Chebyshev networks with handcrafted (HL) and learned Laplacians (Our), and using totally learned Laplacians (TLL). These performances are shown for $K \in \{2, 4, 8\}$ and for different parametrizations of the Laplacians including differential (COMB), and non differential (NDRW, NDN) as well as their combinations (DRW, DN); see again Table. 1. Note that both symmetry and orthogonality constraints are used in these results.

Laplacians Settings		Differential	Non-Differential		Combined	
		COMB	NDRW	NDN	DRW	DN
$K = 2$	HL	85.9130	85.3913	85.5652	85.3913	84.8695
	TLL	85.5652	86.4348	85.7391	85.3913	86.0869
	Our	85.3913	85.7391	85.5652	85.5652	85.7391
$K = 4$	HL	86.4348	84.1739	85.9130	84.0000	84.5217
	TLL	84.3478	85.3913	86.4347	85.0435	85.5652
	Our	85.2174	85.3913	85.7391	87.1304	87.3043
$K = 8$	HL	85.2174	83.8261	86.0869	84.6957	85.7391
	TLL	84.5217	85.5652	85.7391	85.0435	84.8695
	Our	84.6957	86.9565	86.7826	84.6957	84.5217

TABLE 3
Same caption as Table. 2 on the FPHA database.

Dataset	Constraints		Differential	Non-Differential		Combined		Avg. perf.
	Sym	Orth	COMB	NDRW	DRW	NDN	DN	
SBU	\times	\times	90.76	98.46	98.46	96.92	98.46	96.61
	\checkmark	\times	95.38	100.0	98.46	98.46	98.46	98.15
	\times	\checkmark	95.38	96.92	98.46	96.92	98.46	97.23
	\checkmark	\checkmark	98.46	100.00	98.46	98.46	98.46	98.76
Avg.	-	-	95.00	98.84	98.46	97.69	98.46	-
FPHA	\times	\times	79.30	85.21	86.60	86.78	86.43	84.86
	\checkmark	\times	84.00	85.73	85.73	86.43	86.08	85.60
	\times	\checkmark	83.13	85.39	85.73	86.78	86.78	85.56
	\checkmark	\checkmark	85.21	85.39	85.73	87.13	87.30	86.15
Avg.	-	-	82.91	85.43	85.95	86.78	86.65	-

TABLE 4
Ablation study on SBU and FPHA databases, when symmetry (sym) and orthogonality (orth) are taken separately and when combined (in these results $K = 4$). Avg stands for average performances.

6 CONCLUSION

In this paper, we introduce a novel Chebyshev-based Laplacian design for graph convolutional networks (GCNs). The learned Laplacian operators capture the most influencing interactions between body parts in skeleton-based action recognition. The strength of our method resides in its ability to learn shared Laplacians which are embedded into a Chebyshev polynomial basis that allows increasing the discrimination power of our graph representations. In contrast to many existing networks, the parameters of our GCN are interpretable as their design is constrained “by construction” and this also acts as a regularizer that mitigates overfitting. Indeed, our proposed parametrization — together with Laplacian weight sharing, symmetry and orthogonality — enhance the representational power of our learned GCNs without increasing their actual number of the training parameters. Several Laplacian operators are also considered including differential and non-differential ones which model the statistical properties of the learned graph representations, and when combined, they further enhance the performances of action recognition. Extensive experiments, conducted on standard databases (namely SBU and FPHA) show a clear gain of our design w.r.t. different handcrafted and (other) learned Laplacians, as well as the related work in skeleton-based action recognition.

As a future work, we are currently investigating the extension of our method to other applications relying on symmetric positive definite (SPD) matrices in order to aggregate the convolutional features on SPD manifolds [18], [21], [22], [24].

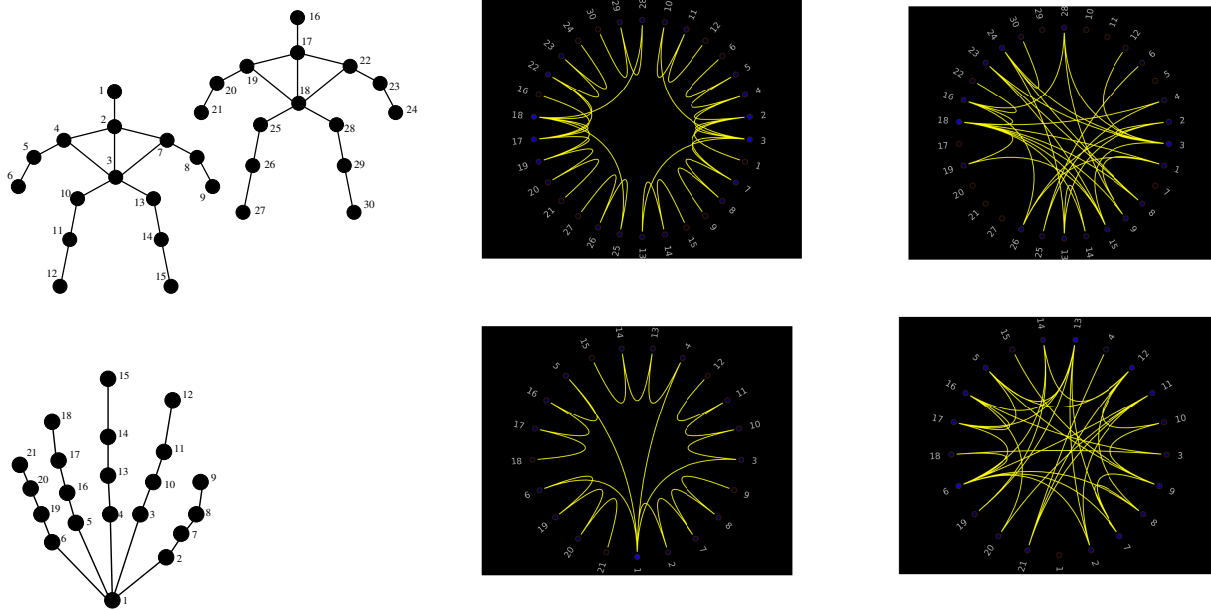


Fig. 3. This figure shows original skeletons (left) with their intrinsic node-to-node relationships useful for *individual identification* (middle), and an example of the adjacency matrix associated to the learned Laplacian which shows the extrinsic node-to-node relationships found to be the most discriminating for *skeleton-based action recognition* when using our proposed method (the exact setting corresponds to Tables 2 and 3, using NDRW for SBU and DN for FPHA both with $K = 4$). (Better to zoom the PDF version to view the learned node-to-node relationships).

Method		Accuracy (%)
Raw Position [134]	CVPRW 2012	49.7
Joint feature [62]	ICMEW 2014	86.9
CHARM [64]	ICCV2015	86.9
H-RNN [29]	CVPR 2015	80.4
ST-LSTM [31]	ECCV 2016	88.6
Co-occurrence-LSTM [59]	AAAI 2016	90.4
STA-LSTM [32]	AAAI 2017	91.5
ST-LSTM + Trust Gate [31]	ECCV 2016	93.3
VA-LSTM [33]	ICCV 2017	97.6
GCA-LSTM [151]	TIP 2018	94.9
Riemannian manifold. traj [149]	PAMI 2018	93.7
DeepGRU [136]	ISVC 2019	95.7
RHCN + ACSC + STUFE [46]	WACV 2020	98.7
Multi-Laplacians (ML baseline)		98.4
Our best (table 2)		100

TABLE 5
Comparison against state of the art methods using the SBU database.

REFERENCES

- [1] Kumar, Sandeep, et al. "A unified framework for structured graph learning via spectral constraints." *JMLR* 21.22 (2020): 1-60.
- [2] Khalil, Elias, et al. "Learning combinatorial optimization algorithms over graphs." In *NIPS*, 2017.
- [3] M. Jiu and H. Sahbi, "Semi supervised deep kernel design for image annotation," in *ICASSP*, 2015.
- [4] Prates, Marcelo, et al. "Learning to solve NP-complete problems: A graph neural network for decision TSP." In *AAAI*. Vol. 33. 2019.
- [5] B. Padeloup, V. Gripon, G. Mercier, D. Pastor, and M. G. Rabbat. Characterization and inference of graph diffusion processes from observations of stationary signals. *IEEE Transactions on Signal and Information Processing over Networks*, 2017.
- [6] M. Jiu and H. Sahbi, "Laplacian deep kernel learning for image annotation," in *ICASSP*, 2016.
- [7] D. Thanou, X. Dong, D. Kressner, and P. Frossard. Learning heat diffusion graphs. *IEEE Transactions on Signal and Information Processing over Networks*, 3(3):484-499, 2017.

Method	Color	Depth	Pose	Accuracy (%)
Two stream-color [137]	✓	✗	✗	61.56
Two stream-flow [137]	✓	✗	✗	69.91
Two stream-all [137]	✓	✗	✗	75.30
HOG2-depth [139]	✗	✓	✗	59.83
HOG2-depth+pose [139]	✗	✓	✓	66.78
HON4D [140]	✗	✓	✗	70.61
Novel View [141]	✗	✓	✗	69.21
1-layer LSTM [59]	✗	✗	✓	78.73
2-layer LSTM [59]	✗	✗	✓	80.14
Moving Pose [142]	✗	✗	✓	56.34
Lie Group [38]	✗	✗	✓	82.69
HBRNN [29]	✗	✗	✓	77.40
Gram Matrix [143]	✗	✗	✓	85.39
TF [145]	✗	✗	✓	80.69
JOULE-color [146]	✓	✗	✗	66.78
JOULE-depth [146]	✗	✓	✗	60.17
JOULE-pose [146]	✗	✗	✓	74.60
JOULE-all [146]	✓	✓	✓	78.78
Huang et al. [19]	✗	✗	✓	84.35
Huang et al. [91]	✗	✗	✓	77.57
Our best (table 3)	✗	✗	✓	87.3

TABLE 6

Comparison against state of the art methods using the FPHA database.

- [8] Y. Li, R. Yu, C. Shahabi, and Y. Liu, "Diffusion convolutional recurrent neural network: Data-driven traffic forecasting," in Proc. of ICLR, 2018.
- [9] Yaguang Li, Chuizheng Meng, Cyrus Shahabi, Yan Liu. Structure-informed Graph Auto-encoder for Relational Inference and Simulation. ICML, 2019
- [10] M. Jiu and H. Sahbi, "Nonlinear deep kernel learning for image annotation," *IEEE Transactions on Image Processing*, vol. 26(4), 2017.
- [11] T Kipf, E Fetaya, KC Wang, M Welling, R Zemel. Neural Relational Inference for Interacting Systems. ICML, 2018
- [12] Ferran Alet, Adarsh K. Jeewajee, Maria Bauza, Alberto Rodriguez, Tomas Lozano-Perez, Leslie Pack Kaelbling. Graph Element Networks: adaptive, structured computation and memory. ICML, 2018
- [13] H. Sahbi, L. Ballan, G. Serra, A. DelBimbo. (2012). Context-dependent logo matching and recognition. *IEEE Transactions on Image Processing*, 22(3), 1018-1031.
- [14] Alet, F., Lozano-Perez, T., and Kaelbling, L. P. Modular meta-learning. In Proceedings of The 2nd Conference on Robot Learning, pp. 856-868, 2018.
- [15] Luca Franceschi and Mathias Niepert and Massimiliano Pontil and Xiao He. Learning Discrete Structures for Graph Neural Networks. ICML, 2019
- [16] H. Sahbi and F. Fleuret. Scale-invariance of support vector machines based on the triangular kernel. Diss. INRIA, 2002.
- [17] Yu Chen, Lingfei Wu, Mohammed J. Zaki. Deep Iterative and Adaptive Learning for Graph Neural Networks. AAAI 2020 Workshop on Deep Learning on Graphs: Methodologies and Applications (AAAI DLGMA 2020)
- [18] T. Zhang, W. Zheng, Z. Cui, and C. Li. Deep Manifold-to-Manifold Transforming Network. CoRR, abs/1705.10732, 2017.
- [19] Z. Huang and L. V. Gool. A Riemannian Network for SPD Matrix Learning. In AAAI, pages 2036–2042, 2017.
- [20] H. Sahbi. Coarse-to-fine deep kernel networks. Proceedings of the IEEE International Conference on Computer Vision, 1131-1139, 2017.
- [21] M. Harandi, M. Salzmann, and R. Hartley. Dimensionality Reduction on SPD Manifolds: The Emergence of Geometry-Aware Methods. TPAMI, 40:48–62, 2018.
- [22] Z. Huang, R. Wang, X. Li, W. Liu, S. Shan, L. V. Gool, and X. Chen. Geometry-Aware Similarity Learning on SPD Manifolds for Visual Recognition. *IEEE Transactions on Circuits and Systems for Video Technology*, 28(10):2513–2523, 2018.
- [23] N. Bourdis, D. Marraud, H. Sahbi. "Constrained optical flow for aerial image change detection." 2011 IEEE International Geoscience and Remote Sensing Symposium. IEEE, 2011.
- [24] Z. Huang, R. Wang, S. Shan, X. Li, and X. Chen. Log-euclidean Metric Learning on Symmetric Positive Definite Manifold with Application to Image Set Classification. In ICML, pages 720–729, 2015.
- [25] A. Mazari and H. Sahbi. MLGCN: Multi-Laplacian Graph Convolutional Networks for Human Action Recognition. BMVC. 2019.
- [26] S. Yan, Y. Xiong, and D. Lin. Spatial temporal graph convolutional networks for skeleton-based action recognition. arXiv preprint arXiv:1801.07455, 2018
- [27] H. Sahbi and X. Li. "Context-based support vector machines for interconnected image annotation." Asian Conference on Computer Vision. Springer, Berlin, Heidelberg, 2010.
- [28] C. Li, Q. Zhong, D. Xie, and S. Pu. Co-occurrence feature learning from skeleton data for action recognition and detection with hierarchical aggregation. arXiv preprint arXiv:1804.06055, 2018.

- [29] Y. Du, W. Wang, and L. Wang. Hierarchical recurrent neural network for skeleton based action recognition. In IEEE Conference on Computer Vision and Pattern Recognition, pages 1110–1118, 2015.
- [30] H. Sahbi. “Kernel-based Graph Convolutional Networks”. IAPR ICPR. 2021.
- [31] J. Liu, A. Shahroudy, D. Xu, and G. Wang. Spatio-temporal LSTM with trust gates for 3D human action recognition. In European Conference on Computer Vision, pages 816–833. Springer, 2016
- [32] S. Song, C. Lan, J. Xing, W. Zeng, and J. Liu. An end-to-end spatio-temporal attention model for human action recognition from skeleton data. In AAAI Conference on Artificial Intelligence, volume 1, pages 4263–4270, 2017
- [33] P. Zhang, C. Lan, J. Xing, W. Zeng, J. Xue, and N. Zheng. View adaptive recurrent neural networks for high performance human action recognition from skeleton data. arXiv preprint arXiv:1703.08274, 2017.
- [34] F. Yuan, G-S. Xia, H. Sahbi, V. Prinet. Mid-level Features and Spatio-Temporal Context for Activity Recognition. Pattern Recognition. volume 45, number 12, 4182-4191, 2012
- [35] S. Zhang, X. Liu, and J. Xiao. On geometric features for skeleton-based action recognition using multilayer lstm networks. In Winter Conference on Applications of Computer Vision, pages 148–157. IEEE, 2017
- [36] H. Sahbi, D. Geman, N. Boujemaa. "Face detection using coarse-to-fine support vector classifiers." Proceedings. International Conference on Image Processing. Vol. 3. IEEE, 2002.
- [37] I. Lee, D. Kim, S. Kang, and S. Lee. Ensemble deep learning for skeleton-based action recognition using temporal sliding lstm networks. In IEEE International Conference on Computer Vision, pages 1012–1020, 2017.
- [38] R. Vemulapalli, F. Arrate, and R. Chellappa. Human action recognition by representing 3D skeletons as points in a Lie group. In IEEE Conference on Computer Vision and Pattern Recognition, pages 588–595, 2014
- [39] L. Xia, C.-C. Chen, and J. K. Aggarwal. View invariant human action recognition using histograms of 3D joints. In IEEE Conference on Computer Vision and Pattern Recognition Workshop, pages 20–27. IEEE, 2012.
- [40] H. Sahbi, “Imageclef annotation with explicit context-aware kernel maps,” *International Journal of Multimedia Information Retrieval*, pp. 113–128, 2015.
- [41] X. Yang and Y. Tian. Effective 3D action recognition using eigenjoints. Journal of Visual Communication and Image Representation, 25(1):2–11, 2014.
- [42] Q. Ke, M. Bennamoun, S. An, F. Sohel, and F. Boussaid. A new representation of skeleton sequences for 3D action recognition. In IEEE Conference on Computer Vision and Pattern Recognition Workshop, pages 4570–4579. IEEE, 2017.
- [43] L. Keselman, J. I. Woodfill, A. Grunnet-Jepsen, and A. Bhowmik. Intel RealSense stereoscopic depth cameras. arXiv preprint arXiv:1705.05548, 2017
- [44] H. Sahbi. "CNRS-TELECOM ParisTech at ImageCLEF 2013 Scalable Concept Image Annotation Task: Winning Annotations with Context Dependent SVMs." CLEF (Working Notes). 2013.
- [45] Z. Zhang. Microsoft Kinect sensor and its effect. IEEE Multimedia, 19(2):4–10, 2012.
- [46] T. Jiang, T. Huang and Y. Tian. Global Co-occurrence Feature Learning and Active Coordinate System Conversion for Skeleton-based Action Recognition. In Winter Conference on Applications of Computer Vision, pages 586-594. IEEE, 2020.
- [47] B. Li, X. Li, Z. Zhang, and F. Wu. Spatio-temporal graph routing for skeleton-based action recognition. AAAI Conference on Artificial Intelligence, 2019
- [48] H. Sahbi, J.-Y. Audibert, and R. Keriven, “Context-dependent kernels for object classification,” *IEEE Transactions on Pattern Analysis and Machine Intelligence*, vol. 33, pp. 699–708, 2011.
- [49] P. Wang, W. Li, Z. Gao, J. Zhang, C. Tang, and P. O. Ogunbona. Action recognition from depth maps using deep convolutional neural networks. IEEE Transactions on Human Machine Systems, 46(4):498–509, 2015.
- [50] P. Wang, W. Li, P. Ogunbona, J. Wan, and S. Escalera. Rgb-d-based human motion recognition with deep learning: A survey. Computer Vision and Image Understanding, 171:118–139, 2018.
- [51] M. Liu and J. Yuan. Recognizing human actions as the evolution of pose estimation maps. In IEEE Conference on Computer Vision and Pattern Recognition, 2018.
- [52] L. Wang, H. Sahbi. Directed Acyclic Graph Kernels for Action Recognition. Proceedings of the IEEE International Conference on Computer Vision. 2013.
- [53] Z. Cao, T. Simon, S.-E. Wei, and Y. Sheikh. Realtime multiperson 2D pose estimation using part affinity fields. In IEEE Conference on Computer Vision and Pattern Recognition Workshop, pages 7291–7299, 2017.
- [54] Y. Wen, L. Gao, H. Fu, F. Zhang, and S. Xia. Graph CNNs with motif and variable temporal block for skeleton-based action recognition. AAAI Conference on Artificial Intelligence, 2019.
- [55] D. K. Duvenaud, D. Maclaurin, J. Iparraguirre, R. Bombarell, T. Hirzel, A. Aspuru-Guzik, and R. P. Adams. Convolutional networks on graphs for learning molecular fingerprints. In Conference on Neural Information Processing Systems, pages 2224–2232, 2015.
- [56] M. Henaff, J. Bruna, and Y. LeCun. Deep convolutional networks on graph-structured data. arXiv preprint arXiv:1506.05163, 2015.
- [57] D. I. Shuman, S. K. Narang, P. Frossard, A. Ortega, and P. Vandergheynst. The emerging field of signal processing on graphs: Extending high-dimensional data analysis to networks and other irregular domains. IEEE Signal Processing Magazine, 30(3):83–98, 2013.
- [58] L. Wang, H. Sahbi. Bags-of-Daglets for Action Recognition. IEEE International Conference on Image Processing (ICIP), 2014.
- [59] W. Zhu, C. Lan, J. Xing, W. Zeng, Y. Li, L. Shen, and X. Xie. Co-occurrence feature learning for skeleton based action recognition using regularized deep LSTM networks In AAAI Conference on Artificial Intelligence, volume 2, page 6, 2016.
- [60] K. Yun, J. Honorio, D. Chattopadhyay, T. L. Berg, and D. Samaras. Two-person interaction detection using body pose features and multiple instance learning. In IEEE Conference on Computer Vision and Pattern Recognition Workshop, 2012.
- [61] H. Sahbi and F. Fleuret. Kernel methods and scale invariance using the triangular kernel. Diss. INRIA, 2004.
- [62] Y. Ji, G. Ye, and H. Cheng. Interactive body part contrast mining for human interaction recognition. In IEEE International Conference on Multimedia and Expo Workshop, pages 1–6. IEEE, 2014.
- [63] H Sahbi. Kernel PCA for similarity invariant shape recognition. Neurocomputing 70 (16-18), 3034-3045
- [64] W. Li, L. Wen, M. Choo Chuah, and S. Lyu. Category-blind human action recognition: A practical recognition system. In IEEE International Conference on Computer Vision, pages 4444–4452, 2015.

- [65] L. Shi, Y. Zhang, J. Cheng, and H. Lu. Non-Local Graph Convolutional Networks for Skeleton-Based Action Recognition. CoRR, abs/1805.07694, 2018
- [66] S. Yan, Y. Xiong, and D. Lin. Spatial Temporal Graph Convolutional Networks for Skeleton-Based Action Recognition. In AAAI, pages 7444–7452, 2018.
- [67] C. Li, Z. Cui, W. Zheng, C. Xu, and J. Yang. Spatio-Temporal Graph Convolution for Skeleton Based Action Recognition. In AAAI, pages 3482–3489, 2018.
- [68] J. Wang, Z. Liu, Y. Wu, and J. Yuan. Mining Actionlet Ensemble for Action Recognition with Depth Cameras. In CVPR, pages 1290–1297, 2012.
- [69] XS. Nguyen, L. Brun, O. Lezoray and S. Bougleux. A neural network based on SPD manifold learning for skeleton-based hand gesture recognition. In IEEE International Conference on Computer Vision and Pattern Recognition, CVPR, 2019.
- [70] P. Vo and H. Sahbi, "Transductive kernel map learning and its application to image annotation," in *BMVC*, 2007.
- [71] J. Luo, W. Wang, and H. Qi. Group Sparsity and Geometry Constrained Dictionary Learning for Action Recognition from Depth Maps. In ICCV, pages 1809–1816, Dec 2013.
- [72] Q. D. Smedt, H. Wannous, and J. Vandeborre. Skeleton-Based Dynamic Hand Gesture Recognition. In CVPRW, pages 1206–1214, June 2016.
- [73] X. Yang and Y. L. Tian. EigenJoints-based Action Recognition Using Naive-Bayes-Nearest-Neighbor. In CVPRW, pages 14–19, 2012
- [74] N. Bourdis, D. Marraud, H. Sahbi. "Camera pose estimation using visual servoing for aerial video change detection." 2012 IEEE International Geoscience and Remote Sensing Symposium. IEEE, 2012.
- [75] G. Evangelidis, G. Singh, and R. Horaud. Skeletal Quads: Human Action Recognition Using Joint Quadruples. In ICPR, pages 4513–4518, 2014.
- [76] C. Wang, Y. Wang, and A. L. Yuille. An Approach to Pose Based Action Recognition. In CVPR, pages 915–922, 2013
- [77] R. Girshick. Fast R-CNN. In ICCV, pages 1440–1448, 2015
- [78] K. He, X. Zhang, S. Ren, and J. Sun. Deep Residual Learning for Image Recognition. In CVPR, pages 770–778, June 2016.
- [79] A. Krizhevsky, I. Sutskever, and G. E. Hinton. ImageNet Classification with Deep Convolutional Neural Networks. In NIPS, pages 1097–1105, 2012.
- [80] M. Liu, H. Liu, and C. Chen. Enhanced Skeleton Visualization for View Invariant Human Action Recognition. Pattern Recognition, 68:346–362, 2017.
- [81] E. Benhaim, H. Sahbi and G. Vitte. Designing relevant features for visual speech recognition. 2013 IEEE International Conference on Acoustics, Speech and Signal Processing. IEEE, 2013.
- [82] P. Wang, Z. Li, Y. Hou, and W. Li. Action Recognition Based on Joint Trajectory Maps Using Convolutional Neural Networks. In ACM MM, pages 102–106, 2016.
- [83] H. Wang and L. Wang. Modeling Temporal Dynamics and Spatial Configurations of Actions Using Two-Stream Recurrent Neural Networks. CVPR, pages 3633–3642, 2017.
- [84] J. Liu, G. Wang, P. Hu, L.-Y. Duan, and A. C. Kot. Global Context-Aware Attention LSTM Networks for 3D Action Recognition. In CVPR, pages 3671–3680, 2017.
- [85] Q. Oliveau, H. Sahbi. Learning attribute representations for remote sensing ship category classification. IEEE Journal of Selected Topics in Applied Earth Observations and Remote Sensing, 2017.
- [86] J. C. Nez, R. Cabido, J. J. Pantrigo, A. S. Montemayor, and J. F. Vlez. Convolutional Neural Networks and Long Short-Term Memory for Skeleton-based Human Activity and Hand Gesture Recognition. Pattern Recognition, 76(C):80–94, 2018.
- [87] A. Shahroudy, J. Liu, T. T. Ng, and G. Wang. NTU RGB+D: A Large Scale Dataset for 3D Human Activity Analysis. In CVPR, pages 1010–1019, 2016.
- [88] J. Weng, M. Liu, X. Jiang, and J. Yuan. Deformable Pose Traversal Convolution for 3D Action and Gesture Recognition. In ECCV, 2018.
- [89] S. Thiemert, H. Sahbi, and M. Steinebach, "Applying interest operators in semi-fragile video watermarking," in *Security, Steganography, and Watermarking of Multimedia Contents VII*, vol. 5681. International Society for Optics and Photonics, 2005, pp. 353–363.
- [90] Z. Huang, C. Wan, T. Probst, and L. V. Gool. Deep Learning on Lie Groups for Skeleton-Based Action Recognition. In CVPR, pages 6099–6108, 2017.
- [91] Z. Huang, J. Wu, and L. V. Gool. Building Deep Networks on Grassmann Manifolds. In AAAI, pages 3279–3286, 2018
- [92] I. Goodfellow, Y. Bengio, and A. Courville. Deep learning. MIT press, 2016.
- [93] H. Sahbi, J.-Y. Audibert and R. Keriven. "Graph-cut transducers for relevance feedback in content based image retrieval." 2007 IEEE 11th International Conference on Computer Vision. IEEE, 2007.
- [94] J. Bruna, W. Zaremba, A. Szlam, Y. LeCun. Spectral networks and locally connected networks on graphs. arXiv preprint arXiv:1312.6203 (2013)
- [95] M. Defferrard, X. Bresson, P. Vandergheynst. Convolutional neural networks on graphs with fast localized spectral filtering. In NIPS, 3844-3852 (2016)
- [96] W. Huang, T. Zhang, Y. Rong, J. Huang. Adaptive sampling towards fast graph representation learning. In NIPS. pp. 4558-4567 (2018)
- [97] T.N. Kipf, M. Welling. Semi-supervised classification with graph convolutional networks. arXiv preprint arXiv:1609.02907 (2016)
- [98] F. Monti, D. Boscaini, J. Masci, E. Rodola, J. Svoboda, M.M. Bronstein. Geometric deep learning on graphs and manifolds using mixture model cnns. In CVPR, pp. 5115–5124 (2017)
- [99] M. Gori, G. Monfardini, F. Scarselli. A new model for learning in graph domains. In IEEE IJCNN, vol. 2, pp. 729–734, 2005.
- [100] A. Micheli. Neural network for graphs: A contextual constructive approach. IEEE TNN 20(3), 498?511 (2009)
- [101] F. Scarselli, M. Gori, A.C. Tsoi, M. Hagenbuchner, G. Monfardini. The graph neural network model. IEEE TNN 20(1), 61–80, 2008.
- [102] Z. Wu, S. Pan, F. Chen, G. Long, C. Zhang, P.S. Yu. A comprehensive survey on graph neural networks. arXiv:1901.00596 (2019).
- [103] W. Hamilton, Z. Ying, J. Leskovec. Inductive representation learning on large graphs. In NIPS. pp. 1024–1034 (2017)
- [104] H. Sahbi, D. Geman. A hierarchy of support vector machines for pattern detection. Journal of Machine Learning Research 7.Oct (2006): 2087-2123.

- [105] R. Levie, F. Monti, X. Bresson, M.M. Bronstein. Cayleynets: Graph convolutional neural networks with complex rational spectral filters. *IEEE Transactions on Signal Processing* 67(1), 97–109 (2018)
- [106] J. Chen, T. Ma, C. Xiao. Fastgcn: fast learning with graph convolutional networks via importance sampling. *arXiv preprint arXiv:1801.10247* (2018)
- [107] Z. Chenyi and Q. Ma. Dual graph convolutional networks for graph-based semi-supervised classification. *Proceedings of WWW*, 2018.
- [108] A. Dutta and H. Sahbi. "High order stochastic graphlet embedding for graph-based pattern recognition." *arXiv preprint arXiv:1702.00156* (2017).
- [109] W. Huang, T. Zhang, Y. Rong, J. Huang. Adaptive sampling towards fast graph representation learning. In *NIPS*. pp. 4558-4567 (2018)
- [110] D. Slepian. Some comments on Fourier analysis, uncertainty and modeling. In *Society for Industrial and Applied Mathematics (SIAM review)*, 1983
- [111] F. Chung. *Spectral graph theory*. American Mathematical Soc.. 1997.
- [112] J. Atwood, D. Towsley. Diffusion-convolutional neural networks. In *NIPS*, pp. 1993–2001 (2016)
- [113] H. Gao, Z. Wang, S. Ji. Large-scale learnable graph convolutional networks. In the 24th ACM SIGKDD International Conference on Knowledge Discovery & Data Mining. pp. 1416–1424. ACM (2018)
- [114] M. Niepert, M. Ahmed, K. Kutzkov. Learning convolutional neural networks for graphs. In *ICML*, pp. 2014-2023 (2016)
- [115] M. Ferecatu and H. Sahbi. MultiView object matching and tracking using canonical correlation analysis. *16th IEEE International Conference on Image Processing (ICIP)*, 2109-2112, 2009.
- [116] J. Zhang, X. Shi, J. Xie, H. Ma, I. King, D.Y. Yeung. Gaan: Gated attention networks for learning on large and spatiotemporal graphs. *arXiv:1803.07294* (2018)
- [117] X. Dong, D. Thanou, P. Frossard, and P. Vandergheynst, Learning Laplacian matrix in smooth graph signal representations, *IEEE Trans. Signal Processing*, vol. 64, no. 23, pp. 6160-6173, 2016.
- [118] N. Boujemaa, F. Fleuret, V. Gouet, H. Sahbi. (2004, January). Visual content extraction for automatic semantic annotation of video news. In the proceedings of the SPIE Conference, San Jose, CA (Vol. 6).
- [119] S.P. Chepuri, S. Liu, G. Leus, and A.O. Hero, Learning sparse graphs under smoothness prior, in *Proc. of ICASSP*, 2017, pp. 6508-6512.
- [120] H.E. Egilmez, E. Pavez, and A. Ortega, Graph learning from data under structural and laplacian constraints, *arXiv preprint arXiv:1611.05181*, 2016.
- [121] V. Kalofolias, How to learn a graph from smooth signals, in *Proc. of the conf. on Artificial Intelligence and Statistics*, 2016, pp. 920-929.
- [122] M. Belkin and P. Niyogi. Lapl eigenmaps for dimensionality reduction and data representation. *Neural computation* 15.6 (2003): 1373-1396.
- [123] X. Dong, D. Thanou, M. Rabbat, and P. Frossard, Learning graphs from data: A signal representation perspective, *arXiv preprint arXiv:1806.00848*, 2018.
- [124] L. Wang, H. Sahbi. *Nonlinear CrossView Sample Enrichment for Action Recognition*. European Conference on Computer Vision. Springer, 2014.
- [125] S.I. Daitch, J.A. Kelner, and D.A. Spielman, Fitting a graph to vector data, in *Proc. of ICML*, 2009, pp. 201-208.
- [126] S. Sardellitti, S. Barbarossa, and P. Di Lorenzo, Graph topology inference based on transform learning, in *Proc. of the Global Conf. on Signal and Information Processing*, 2016, pp. 356-360.
- [127] B. Le Bars, P. Humbert, L. Oudre and A. s Kalogeratos. Learning Laplacian Matrix from Bandlimited Graph Signals. In *ICASSP*, 2019
- [128] S. Sardellitti, S. Barbarossa, and P. Di Lorenzo. Graph topology inference based on sparsifying transform learning. *IEEE TSP*, 67(7), 2019.
- [129] H. Sahbi and N. Boujemaa. "From coarse to fine skin and face detection." *Proceedings of the eighth ACM international conference on Multimedia*. 2000.
- [130] D. Valsesia, G. Fracastoro, and E. Magli, Sampling of graph signals via randomized local aggregations, *arXiv preprint arXiv:1804.06182*, 2018.
- [131] W. Li, Y. Lu, K. Zheng, H. Liao, C. Lin, J. Luo & Miao, S. Structured Landmark Detection via Topology-Adapting Deep Graph Learning. *arXiv preprint arXiv:2004.08190*. 2020
- [132] H. Sahbi, JY. Audibert, J. Rabarisoa, R. Keriven. Object recognition and retrieval by context dependent similarity kernels. *International Workshop on Content-Based Multimedia Indexing*, 216-223, 2008.
- [133] G. Garcia-Hernando, S. Yuan, S. Baek, and T.-K. Kim. First- Person Hand Action Benchmark with RGB-D Videos and 3D Hand Pose Annotations. In *CVPR*, 2018.
- [134] K. Yun, J. Honorio, D. Chattopadhyay, T.L. Berg, and D. Samaras. Two-person interaction detection using body pose features and multiple instance learning. In *IEEE Conference on Computer Vision and Pattern Recognition Workshop*, 2012.
- [135] M. Meshry, M.E. Hussein, and M. Turki. "Linear-time online action detection from 3d skeletal data using bags of gesturelets." *2016 IEEE Winter Conference on Applications of Computer Vision (WACV)*. IEEE, 2016.
- [136] M. Maghoumi, JJ. LaViola Jr. DeepGRU: Deep Gesture Recognition Utility. In *arXiv preprint arXiv:1810.12514*, 2018
- [137] C. Feichtenhofer, A. P., and A. Zisserman. Convolutional Two-Stream Network Fusion for Video Action Recognition. *CVPR*, pages 1933-1941, 2016.
- [138] H. Sahbi, "Explicit context-aware kernel map learning for image annotation," in *ICVS*, 2013.
- [139] E. Ohn-Bar and M.M. Trivedi. Hand Gesture Recognition in Real Time for Automotive Interfaces: A Multimodal Vision- Based Approach and Evaluations. *IEEE Transactions on Intelligent Transportation Systems*, 15(6):2368-2377, 2014.
- [140] O. Oreifej and Z. Liu. HON4D: Histogram of Oriented 4D Normals for Activity Recognition from Depth Sequences. In *CVPR*, pages 716-723, June 2013.
- [141] H. Rahmani and A. Mian. 3D Action Recognition from Novel Viewpoints. In *CVPR*, pages 1506-1515, June 2016.
- [142] M. Zanfir, M. Leordeanu, and C. Sminchisescu. The Moving Pose: An Efficient 3D Kinematics Descriptor for Low-Latency Action Recognition and Detection. In *ICCV*, pages 2752-2759, 2013.
- [143] X. Zhang, Y. Wang, M. Gou, M. Szaier, and O. Camps. Efficient Temporal Sequence Comparison and Classification Using Gram Matrix Embeddings on a Riemannian Manifold. In *CVPR*, pages 4498-4507, 2016.

- [144] M. Jiu and H. Sahbi, "Deep representation design from deep kernel networks," *Pattern Recognition*, vol. 88, pp. 447–457, 2019.
- [145] G. Garcia-Hernando and T.-K. Kim. Transition Forests: Learning Discriminative Temporal Transitions for Action Recognition. In CVPR, pages 407–415, 2017.
- [146] J. Hu, W. Zheng, J. Lai, and J. Zhang. Jointly Learning Heterogeneous Features for RGB-D Activity Recognition. In CVPR, pages 5344–5352, 2015.
- [147] D.P. Kingma, and J. Ba. "Adam: A method for stochastic optimization." arXiv preprint arXiv:1412.6980 (2014).
- [148] R. Ando and T. Zhang. Learning on graph with Laplacian regularization. *Advances in neural information processing systems*, 19, 25-32 (2006).
- [149] A. Kacem, M. Daoudi, B. Ben Amor, S. Berretti, J-Carlos. Alvarez-Paiva. A Novel Geometric Framework on Gram Matrix Trajectories for Human Behavior Understanding. *IEEE Transactions on Pattern Analysis and Machine Intelligence*, 28 September 2018
- [150] M. Jiu and H. Sahbi. Deep kernel map networks for image annotation. *IEEE International Conference on Acoustics, Speech and Signal Processing (ICASSP)*, 2016.
- [151] J. Liu, G. Wang, L. Duan, K. Abdiyeva, and A. C. Kot. Skeleton-based human action recognition with global context-aware attention lstm networks. *IEEE Transactions on Image Processing*, 27(4):1586–1599, April 2018